ACS OMEGA

http://pubs.acs.org/journal/acsodf

Article

# Influence of DMβCD on the Interaction of Copper(II) Complex of 6-Hydroxychromone-3-carbaldehyde-3-hydroxybenzoylhydrazine with *ct*DNA

Horacio Gómez-Machuca,[§] Cinthia Quiroga-Campano,[§] Gerald Zapata-Torres, and Carolina Jullian*

Cite This: *ACS Omega* 2020, 5, 6928−6936

Read Online

ACCESS | Metrics & More | Article Recommendations | Supporting Information

**ABSTRACT:** The interaction mechanism between a scarcely soluble copper(II) complex of Cu(II)-6-hydroxychromone-3-carbaldehyde-(3′-hydroxy)benzoylhydrazone (**CuCHz**) in aqueous solution and its DMβCD complex was studied in the presence of *ct*DNA through spectroscopy and thermodynamic methods. The thermodynamic results indicate that the binding process of the **CuCHz**−DMβCD inclusion complex is a spontaneous process and the inclusion is enthalpy-driven. The binding constants of **CuCHz** and **CuCHz**−DMβCD with *ct*DNA are $2.69 \times 10^3$ and $14.7 \times 10^3$ L mol$^{-1}$, respectively. The stoichiometry of the complex is 1:1, and the determined thermodynamic indicates that the process of binding is spontaneous and entropy-driven. A competitive binding titration with ethidium bromide revealed that **CuCHz** efficiently displaces EB from the EB−DNA system. In addition to the thermal denaturation experiments and docking studies, we can confirm that the mode of binding of this complex to *ct*DNA is intercalation mode. The presence of DMβCD enhances the aqueous solubility of **CuCHz**; nevertheless, the cyclodextrin did not affect the interaction of **CuCHz** with *ct*DNA because the inclusion complex breaks down when it binds with *ct*DNA.

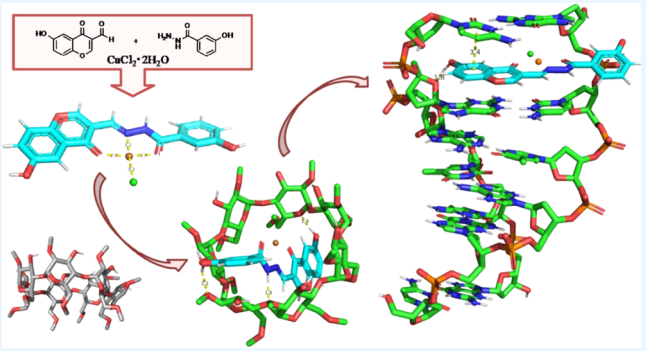


## INTRODUCTION

Design of small molecules that bind and react at specific sequences of deoxyribonucleic acid *ct*DNA is very important in the development of new therapeutic reagents. *ct*DNA is generally the primary intracellular target of anticancer drugs, so the interaction between small molecules and *ct*DNA can often cause *ct*DNA damage in cancer cells, blocking their division with concomitant cell death.[1]

Chromone(1-benzopyran-4-one) moiety as a ligand scaffold represents a class of naturally occurring molecules.[2] They have attracted attention in recent years because of their diverse pharmacological properties such as antimycobacterial, antifungal, anticancer, antioxidant, antihypertensive, and anti-inflammatory effects.[3,4] Transition-metal complexes obtained from 3-formylchromone Schiff bases have still received considerable attention, in view of their chelating ability exhibiting efficient *ct*DNA binding.[5−10] This type of compounds bearing N and O donors has structural similarities to neutral biological systems in which the C═N linkage of azomethine derivatives is essential for their displayed biological activity. Also, it has been demonstrated that this chelating activity is enhanced on chelation with metal atoms due to the increase in the planarity of the intercalators, allowing the insertion of the complexes and their stacking between the base pairs of double-helical *ct*DNA more easier than the free ligands.[7,10] A number of metal complexes (Cu(II), Zn(II), Pd(II), Pt(II), Ni(II), La(III), Ru(II), Sm(III), and Nd(III)) with Schiff base derivative have been reported, and their *ct*DNA-binding properties have been studied.[5−13] Nevertheless, these metal complexes have a disadvantage due to their water solubility, which is still unsatisfactory, restricting their use as anticancer agents.[14,15]

Drug carrier vehicles play an important role in the active transport of drugs in both increasing concentration and effectiveness of drugs at the required site. In this context, cyclodextrins (CDs) play a pivotal role in supramolecular delivery applications due to their nature as macrocyclic hosts, as reported in many drug formulations.[16] CDs are cyclic oligosaccharides with a cagelike structure formed by α-1,4-linked D-glucopyranose units. CDs have the shape of a truncated cone with internal cavities ranging from 5 to 8 Å. The C−H bonds (H-3′, H-5′) on the ring point inward, producing a hydrophobic cavity. In this conformation, electron

**Received:** January 20, 2020
**Accepted:** March 10, 2020
**Published:** March 20, 2020






https://dx.doi.org/10.1021/acsomega.0c00275
*ACS Omega* 2020, 5, 6928−6936

**Scheme 1. One-Pot Synthesis of the Copper(II) Complex of 6-Hydroxychromone-3-carbaldehyde-3-hydroxybenzoylhydrazine (CuCHz)**

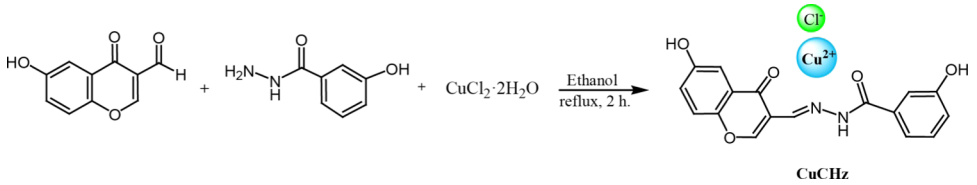


lone pairs belonging to glycosidic oxygens remain toward the interior of the CD cavity, thus increasing the electron density along with the Lewis base character of the latter.[17] Cyclodextrins and modified cyclodextrins form inclusion complexes capable of binding substrates that quickly, selectively, and reversibly act as catalysts in a variety of chemical reactions.[18] It is very well known that hydrophobic molecules and/or some hydrophobic moieties display an increased affinity for CD's cavity in the aqueous solution. In fact, the capability of cyclodextrins to improve and enhance not only the solubility but also the stability of several drugs is known to be mediated through the formation of inclusion complexes.[19] The stability of these inclusion complexes is determined by the fit of the entire or at least the hydrophobic part of the guest molecule. On the other hand, modified cyclodextrin derivatives like methylation of the hydroxyl groups have attracted interest because they have greater water solubility. In this sense, dimethyl-$\beta$-cyclodextrin has been used to include diverse drugs like paclitaxel,[20,21] hydroxymethylnitrofurazone,[22] luteolin,[23] 4-hydroxycoumarin,[24] catechin,[25] (−)-epigallocatechin galate,[26] and morin,[27] improving their complexing ability and stabilization of the incorporated drug. Even though cyclodextrins are recognized by the ability to form such complexes as reported elsewhere (vide supra), reports on drugs that bind to *ct*DNA and solubilized by cyclodextrin are scanty.[28−35] Also, cyclodextrins are recognized to increase the solubility of complexes and/or to modulate the binding of small molecules to *ct*DNA by selectively blocking/orienting the drug upon its binding.

Copper(II) complexes have attracted considerable attention owing to their high affinity for nucleobases and their capability of interacting directly with *ct*DNA that leads to cell cycle arrest and in turn to cell death.[36] Therefore, this study contributes to improving the aqueous solubility of the copper(II)-6-hydroxychromone-3-carbaldehyde-(3′-hydroxy)-benzoylhydrazone (**CuCHz**) complex through inclusion in DM$\beta$CD and also leads to a better understanding of the effect of cyclodextrins on the properties and functionality of drug−*ct*DNA complexes. Different methods were employed to investigate the *ct*DNA-binding ability of **CuCHz**. This included fluorescence titration at different temperatures to determine thermodynamic parameters, fluorescence displacement assays, and thermal denaturation and molecular docking studies.

## RESULTS AND DISCUSSION

**One-Pot Synthesis of Copper(II) Complex (CuCHz).** The mixture of copper(II) chloride dihydrate (4 mmol), 6-hydroxy-chromone-3-carboxaldehyde (2 mmol), and 3-hydroxybenzoylhydrazine (2 mmol) in ethanol was stirred and heated under reflux for 2 h (Scheme 1). The resulting green precipitate, copper(II) complex, was collected by filtration, washed several times with ethanol, and dried overnight at 80 °C. Yield, 82%; mp, 277 °C (decomp.). FTIR ($cm^{-1}$) 3264 ($\nu$ NH), 3436−3092 ($\nu$ OH), 1638 ($\nu$ C═O chromone), 1605 ($\nu$ C═O hydrazone), 1569 ($\nu$ C═N). HRMS ($C_{17}H_{12}Cl_2CuN_2O_5$): $[M-H]^-$ = 457.9292. Anal. calcd for $C_{17}H_{12}Cl_2CuN_2O_5$: C, 44.51%; H, 2.64%; N, 6.11%. Found: C, 43.93%; H, 2.56%; N, 5.91% (Figures S1−S3).

The copper(II) complex is easily soluble in DMF and DMSO; slightly soluble in ethanol, methanol, water, and acetone; and insoluble in benzene and diethyl ether. The UV spectra had a strong band at $\lambda_{max}$ = 260 nm, a medium band at $\lambda_{max}$ = 372 nm, and a weak band at $\lambda_{max}$ = 432 nm. Fluorescence spectra have a maximum at 440 nm with an excitation wavelength of 335 nm with bandwidths for excitation and emission of 5 and 12 nm, respectively. Even though the complex was formed by one-pot synthesis, characterization of **CHz** (6-hydroxychromone-3-carbaldehyde-(3′-hydroxy)-benzoylhydrazone) and the NMR titration curve with Cu(II) was recorded to confirm the complex formation (Figures S4−S9).

The stability of **CuCHz** in the aqueous solution has been studied by observing the UV−vis spectrum and remained unaltered for 24 h. The molar conductivity of the Cu(II) complex is 88.3 S $cm^2$ $mol^{-1}$ in DMSO, showing that it is 1:1 electrolyte, indicating that the chloride anion is out of the coordination sphere as a counter ion.[37] The thermogram show no weight loss up to 250 °C for **CHz** and 200 °C for **CuCHz**, confirming the stability of the copper(II) complex as well as the absence of any water molecule in/out of the coordination sphere (Figure S3). The magnetic moment of the complex **CuCHz** is 1.70 BM, giving an indication of a one-electron paramagnetic $d^9$−Cu(II) center that suggests a square planar complex.[38] The characterization of the obtained complex indicates that the structure is [Cu(CHz)Cl]Cl.

The IR spectra of Cu(II)-6-hydroxychromone-3-carbaldehyde-(3′-hydroxy)benzoylhydrazone (**CuCHz**) show a broad band at around 3000 $cm^{-1}$ due to the presence of OH and NH moieties. Also, a strong band at 1569 $cm^{-1}$ is observed due to the stretching vibration of the $\nu$(C═N) group. This signal was shifted to a lower frequency compared to $\nu$(C═N) of **CHz**, which indicates the coordination of azomethine nitrogen to the metal ion. This shift may be the result of a transfer of the electron density from the donor atom (N) toward the metal center, leading to weakening of the $\nu$(C═N) absorption band. As well, two characteristic carbonyl stretching frequencies are observed at 1638 and 1605 $cm^{-1}$ that are assigned to $\nu(C{=}O)_{chromone}$ and $\nu(C{=}O)_{hydrazone}$, moieties, respectively. The latter signals are shifted to a lower wavenumber compared to the vibration of **CHz**, indicating that both carbonyl oxygen and azomethine nitrogen atoms could participate as an ONO-tridentate ligand[39,40] in the presence of copper. Besides different tautomeric forms that can exist for **CHz**, there is only one structural copper complex that takes place and is definitively that poses two carbonyl groups.


https://dx.doi.org/10.1021/acsomega.0c00275
ACS Omega 2020, 5, 6928−6936

When increased concentrations of DM$\beta$CD are added to the reaction medium containing **CuCHz**, the recorded absorption spectra show only minor changes; however, the effect of DM$\beta$CD on the fluorescence spectra is more pronounced. At pH 7.4, the emission maximum is at 440 nm and the addition of increasing concentrations of DM$\beta$CD from 0 to 2.65 mmol $L^{-1}$ resulted in a corresponding increase in the fluorescence signal with a slight displacement to lower wavenumber (Figure 1). One of the results of formation inclusion complexes, in our

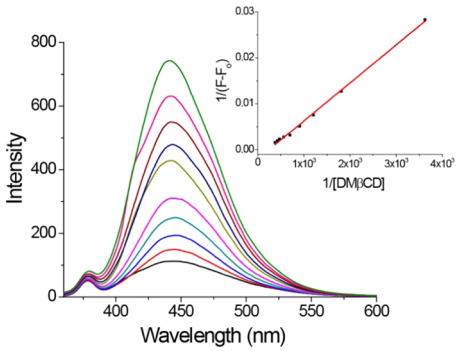


**Figure 1.** Fluorescence intensity of **CuCHz** ($1 \times 10^{-5}$ mol $L^{-1}$) in the presence of various concentrations of DM$\beta$CD ($0.2–2.6 \times 10^{-3}$ mol $L^{-1}$) in phosphate buffer, pH 7.4. Inset: Double reciprocal plot $1/\Delta F$ versus 1/[DM$\beta$CD] obtained from the fluorescence intensities recorded for the **CuCHz**–DM$\beta$CD complexes. $\lambda_{exc}$, 335 nm; $\lambda_{em}$, 440 nm. Excitation and emission bandwidths were set at 5 and 12 nm, respectively.

case **CuCHz** and DM$\beta$CD, is the increase in the observed fluorescence intensity, which could be due to the change in the microenvironment of **CuCHz** as it entered in the cavity of DM$\beta$CD. To determine the stoichiometry of this complex, we analyzed the intensity changes in the emission spectra according to the Benesi–Hildebrand plot,[41] results that confirmed a 1:1 stoichiometry corroborated by a straight line by the continuous variation method (Figure S11).

The association constants, $K_a$, of the inclusion complexes between the Cu(II) complex (**CuCHz**) and cyclodextrin at different temperatures (298, 308, and 318 K) were calculated from the double reciprocal plot, and the results are summarized in Table 1. From Table 1, it is possible to notice

**Table 1. Association Constant ($K_a$) of the CuCHz–DM$\beta$CD Complex at Different Temperatures and Thermodynamic Parameters**

| $T$ (K) | $K_a$ (L $mol^{-1}$) | $\Delta G$ (kJ $mol^{-1}$) | $\Delta H$ (kJ $mol^{-1}$) | $\Delta S$ (kJ $mol^{-1}$ $K^{-1}$) |
|---|---|---|---|---|
| 298 | 240 ± 11 | −13.60 | −11.58 | $6.60 \times 10^{-3}$ |
| 308 | 199 ± 37 | | | |
| 318 | 179 ± 33 | | | |

that the determined association constant for the **CuCHz**–DM$\beta$CD complex decreases when the temperature increases, in total agreement with an exothermic process. This could be thought of as a decreasing degree of interaction occurring at higher temperatures due to the weakening of hydrogen bonds in the heating process.

The thermodynamic parameters ($\Delta G$, $\Delta H$, and $\Delta S$) for the formation of inclusion complexes were determined from the temperature dependence of the apparent formation constants using the classical van't Hoff equation and plotting ln $K$ versus $1/T$

$$\ln K = -\frac{\Delta H^\circ}{RT} + \frac{\Delta S^\circ}{R} \quad (1)$$

where $K$ is the associative binding constant corresponding to various temperatures and $R$ is the gas constant (8.314 J $K^{-1}$ $mol^{-1}$). The standard-state enthalpy change ($\Delta H^\circ$) can be calculated from the slope of the van't Hoff relationship, the standard-state entropy change ($\Delta S^\circ$) can be calculated from the intercept, and the standard-state Gibbs energy change ($\Delta G^\circ$) can be estimated from the following relationship

$$\Delta G = \Delta H - T\Delta S \quad (2)$$

In CD complex formation, several driving forces must be considered, namely, hydrogen bonding formation among hydroxyl groups of CDs and the guest molecules. Also, van der Waals interactions play an important role in host–guest molecules. Hydrophobic and the expulsion of "high energy waters" from the interior of cyclodextrin toward bulk water must be considered. The result of the changes can be noticed in large negative enthalpy and in entropy values (either negative or slightly positive), which can be attributed to strong van der Waals interactions and hydrogen bond formation at the interior of the hydrophobic cavity, leading to guest inclusion without extensive desolvation.[42] According to the values of $\Delta H^\circ$ and $\Delta S^\circ$ given in Table 1, the inclusion process of **CuCHz** with DM$\beta$CD might correspond to an enthalpy-driven process. The negative value of the standard Gibbs energy change ($\Delta G$), which is the result of the interplay of enthalpy and entropy changes, indicates in our case that the formation of the inclusion complex is a spontaneous process.

The electronic structure of the Cu(II) complex was obtained by means of density functional theory (DFT) calculations. The molecular geometry was fully optimized using Gaussian 09 at the B3LYP level. Nonmetal atoms were described with B3LYP/6-31G(d), and Cu(II) atom was treated by B3LYP/LANL2DZ basis sets. The optimized structure is shown in Figure 2a. With this conformation at hand, we used a

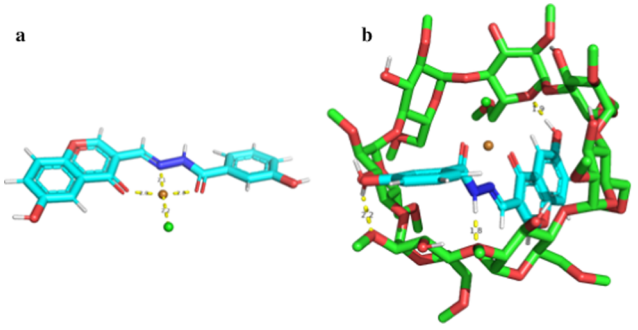


**Figure 2.** (a) Fully optimized molecular geometry of **CuCHz** and (b) molecular structure of the most stable **CuCHz**–DM$\beta$CD complex, as calculated by docking studies.

previously optimized DM$\beta$CD[28] to carried out molecular docking studies using the AutoDock 4.2 version program to determine the most stable structure of the Cu(II) complex. Then, the most stable conformation for the Cu(II) complex was chosen according to the best docking score. According to this result, only one orientation of the guest complex and the host molecule (DM$\beta$CD) was found where the chromone


https://dx.doi.org/10.1021/acsomega.0c00275
ACS Omega 2020, 5, 6928–6936

moiety of **CuCHz** remains toward the primary ring and the benzoyl ring toward the secondary rim. In this attained conformation, it is possible to observe three hydrogen bonds namely, a hydrogen bond between the OH group of benzoyl and 2-$OCH_3$ in the secondary face at 2.2 Å. Another hydrogen bond remains with the anomeric oxygen of the chromone moiety at 1.9 Å toward the primary face of DM*β*CD. The N−H group in that conformation forms a hydrogen bond with the opposite anomeric oxygen at 1.8 Å. In that actual conformation, the complex remains completely embedded in the CD hydrophobic cavity (Figure 2b).

Interaction studies of metal complexes with *ct*DNA are significant for designing new drugs. Spectral changes in absorbance or fluorescence are important to find out the possible mechanism of binding of the compound with *ct*DNA. The absorption spectrum of **CuCHz** forming an inclusion complex with DM*β*CD presents two bands corresponding to 268 and 423 nm. In the presence of an increasing concentration of *ct*DNA, a marked decrease in the absorbance at 423 nm (approximately 33.16%) and a progressive blue shift of 8 nm (Figure S12) are observed, indicative of an interaction between **CuCHz**−DM*β*CD and *ct*DNA, which could be due to a stacking interaction between the aromatic chromophore and the base pair of *ct*DNA.[35,43]

We used fluorescence spectroscopy to analyze the interactions occurring between CuCHz with *ct*DNA, considering the presence (or the absence) of DM*β*CD at fixed concentrations of CuCHz and increased concentrations of *ct*DNA (Figures S13 and S14). In the case of fluorescence, a significant increase in the fluorescence emission is normally observed for intercalation modes of interaction.[44] The degree of freedom of guest molecules, especially rotations, favors the deactivation of excited states. However, when molecule CuCHz, that is used in this study, is bound to *ct*DNA, it becomes rigid, favoring the emission fluorescence with an observed concomitant increase in the emission. Other interactions, namely, electrostatic, hydrogen bonding, or hydrophobic, known to occur in groove binding agents result in a decrease in the fluorescence intensity in the presence of *ct*DNA mainly due to their closeness to the sugar−phosphate backbone.[45] The Cu(II) complex emits weak fluorescence in Tris buffer with a maximum wavelength of about 440 nm. Upon addition of increasing concentrations of *ct*DNA, there is an enhancement in the emission intensity, indicative of a certain type of interaction with *ct*DNA (Figure 3). In the presence of cyclodextrin, the behavior is to some extent alike; there is still an enhancement of fluorescence in the presence of *ct*DNA without a significant shift of the emission wavelength maximum in the aqueous solution. This increase in the emission intensity agrees well with that observed for other intercalators,[46] suggesting that **CuCHz** interacts with *ct*DNA and is protected from solvent water molecules by the hydrophobic environment inside the *ct*DNA helix. Nevertheless, the cyclodextrin complex interacts with *ct*DNA more efficiently, which could be due to the enhancement of the solubility of the Cu(II) complex.

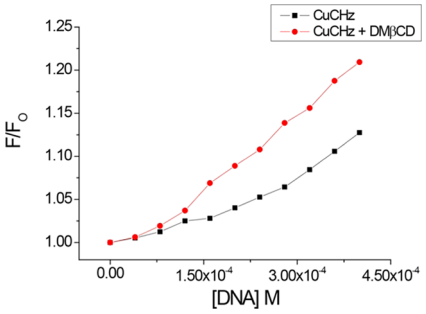


**Figure 3.** Relative changes in the fluorescence intensity ($F/F_0$) of **CuCHz** (10 $\mu$M) and **CuCHz**−DM*β*CD (10 $\mu$M) with the increased addition of *ct*DNA (0−22.5 $\mu$M) in the buffer solution.

To compare the binding strength of both complexes with *ct*DNA, the binding constant, $K_b$, and the number of binding sites, $n$, from the fluorescence spectral changes on titration with *ct*DNA were determined using the following equation

$$\log \frac{F_0 - F}{F} = \log K_b + n \log[Q] \quad (3)$$

where $K_b$ is the binding constant, $n$ is the number of binding sites, $F_0$ is the fluorescence intensity of the small molecule in the absence of *ct*DNA, while $F$ is the fluorescence intensity of the small molecule in the presence of *ct*DNA, and $[Q]$ is the concentration of *ct*DNA. $K_b$ and $n$ are easily calculated from the double logarithm regression curve of $\log(F_0 - F)/F$ versus $\log[Q]$. The values of $K_b$ and $n$ were estimated from the intercept and slope of the plot of $\log \Delta F/F$ versus $\log[Q]$, respectively. The binding constant and the number of binding sites for the interaction between **CuCHz** and *ct*DNA in the absence and presence of cyclodextrin were determined (Table 2). The values of $n$ are approximately 1.3 for both Cu(II) complex (with and without cyclodextrin); this showed a 1:1 stoichiometric interaction of **CuCHz** and *ct*DNA, which indicates the existence of just a single binding site in *ct*DNA for **CuCHz**. The binding constant, $K_b$, of **CuCHz** with *ct*DNA at 298 K was $2.69 \times 10^3$ L $mol^{-1}$ (correlation coefficient, 0.990), and in the presence of cyclodextrin, the $K_b$ value increases to $14.7 \times 10^3$ L $mol^{-1}$ (correlation coefficient, 0.986). It has been reported that cyclodextrin does not cause any DNA cleavage;[47] therefore, DM*β*CD besides enhancing the solubility of **CuCHz** selectively orients the drug molecule upon its binding to *ct*DNA.[28] From these results, we confirm that cyclodextrin is a good delivery nanovehicle for the supply of a drug to target *ct*DNA.

As depicted in Table 2, the $K_b$ values of **CuCHz** on *ct*DNA in the presence of cyclodextrin increase in the range of temperature from 298 to 318 K. This demonstrated that **CuCHz** has a good affinity for *ct*DNA and the stability of the association of **CuCHz** with *ct*DNA growth upon an increase in temperature.

The analysis of thermodynamic parameters including $\Delta G$, $\Delta H$, and $\Delta S$ is one of the effective methods for judging the mode of association of small molecules with biomolecules. As stated before, several interactions can be identified when it comes to describing the binding of drugs to a pharmaceutical target such as DNA, namely, hydrogen bonds, van der Waals forces, and electrostatic and hydrophobic interactions. Enthalpy and entropy changes can be determined when the dependence of $K_b$ with temperature is analyzed by means of the van't Hoff equation (eq 1). Our results are given in Table 2. The sign and magnitude of several thermodynamic parameters associated with individual interactions occurring in the association process of drugs and macromolecules have been given elsewhere.[48,49] Using this description, we observed what kinds of interactions were the predominant ones. When $\Delta H < 0$ or $\Delta H = 0$ and $\Delta S > 0$, the mainly acting force is


https://dx.doi.org/10.1021/acsomega.0c00275
ACS Omega 2020, 5, 6928−6936

Table 2. Binding Constants ($K_b$) of CuCHz and the CuCHz−DM$\beta$CD Complex with *ct*DNA at Different Temperatures and Thermodynamic Parameters of CuCHz−DM$\beta$CD with *ct*DNA

| | $T$ (K) | log $K_b$ | $K_a$ (L mol$^{-1}$) | $n$ | $R$ | $\Delta G$ (kJ mol$^{-1}$) | $\Delta H$ (kJ mol$^{-1}$) | $\Delta S$ (kJ mol$^{-1}$ K$^{-1}$) |
|---|---|---|---|---|---|---|---|---|
| **CuCHz** | 298 | 3.43 | 2690 | 1.29 | 0.990 | | | |
| **CuCHz**−DM$\beta$CD | 298 | 4.17 | 14 791 | 1.33 | 0.986 | −24.76 | 3.58 | $9.20 \times 10^{-2}$ |
| **CuCHz**−DM$\beta$CD | 308 | 4.19 | 15 488 | 1.36 | 0.991 | | | |
| **CuCHz**−DM$\beta$CD | 318 | 4.21 | 16 218 | 1.35 | 0.985 | | | |

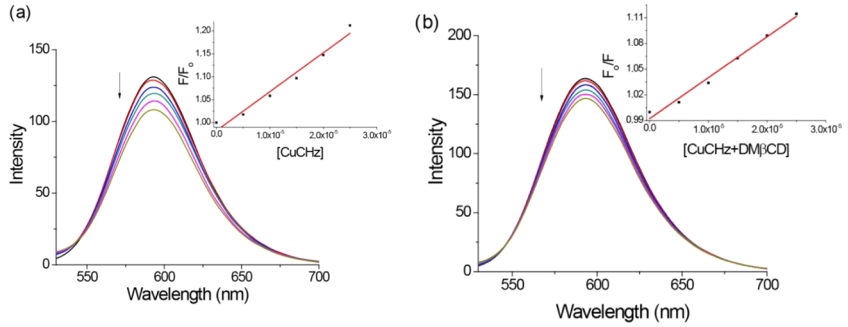


**Figure 4.** Emission spectra of EB (0.33 $\mu$mol L$^{-1}$) bound to *ct*DNA (15 $\mu$mol L$^{-1}$) in the presence of (a) **CuCHz** and (b) **CuCHz**−DM$\beta$CD at different concentrations (0.5−2.5 × 10$^{-5}$ mol L$^{-1}$). Inset: fluorescence quenching curves of EB−*ct*DNA.

electrostatic; when $\Delta H < 0$, $\Delta S < 0$, van der Waals interactions or hydrogen bonds dominate the reaction, and when $\Delta H > 0$, $\Delta S > 0$, the main force is hydrophobic. Thermodynamic parameters obtained are listed in Table 2, where the positive small values 3.58 kJ mol$^{-1}$ for $\Delta H$ and 0.092 kJ mol$^{-1}$ for $\Delta S$ between **CuCHz**−DM$\beta$CD and *ct*DNA indicated that the binding is mainly entropy-driven. This means that the hydrophobic forces play a major role in the binding; nevertheless, due to the low value of the enthalpy change, the other noncovalent interactions cannot be excluded.[50,51] In general, the complex of major/minor groove binding is stabilized by electrostatic, hydrogen bonding, and/or hydrophobic interactions;[52] however, the complex of intercalation, where a planar aromatic chromophore is inserted between two adjacent base pairs in a *ct*DNA helix, is a process that starts with the transfer of the intercalating molecule from a hydrophobic cavity (cyclodextrin) to the hydrophobic space between two adjacent *ct*DNA base pairs and is stabilized by hydrophobic interactions and van der Waals forces.[47] This suggests that entropy and enthalpy processes drive the interaction of **CuCHz**−DM$\beta$CD with *ct*DNA and this binding can be assigned to the intercalation mode.

To test whether the copper complex binds to *ct*DNA via intercalation, ethidium bromide was employed. To check whether the metal complexes have the ability to achieve complexation with *ct*DNA, competitive binding experiments are a valid method.[53] EB was selected as a fluorescence probe because of its known spectral properties, and it is widely used as a fluorescence chromophore marker for *ct*DNA. The fluorescence intensity of the EB−*ct*DNA system is much better than that of free EB due to the strong intercalation between the adjacent *ct*DNA base pairs. If the Cu(II) complex has the same binding mode with *ct*DNA as that of EB, the fluorescence-based competition technique can provide indirect evidence for the *ct*DNA-binding mode. This means that the fluorescence of the EB−*ct*DNA system can be quenched by the addition of a second species that is able to displace the EB molecules.

Competitive binding studies using ethidium bromide bound to *ct*DNA were carried out. Figure 4 shows the variation of emission spectra of *ct*DNA pretreated with EB ([DNA]/[EB] = 1:1) with increasing concentration of the Cu(II) complex in the absence and presence of DM$\beta$CD. A fluorescence decrease of EB−*ct*DNA was observed at the maximum of 593 nm as the concentration of the copper(II) complex increases in the absence and presence of cyclodextrin. The results revealed the quenching of the initial fluorescence intensity about 10 and 18% for **CuCHz** with and without DM$\beta$CD, respectively, and in both situations, the displacement of EB occurs, which indicates that **CuCHz** in both forms could displace EB from the EB−*ct*DNA system.

To further exclude the possible presence of other processes, thermal denaturation properties are investigated. The effect of denatured *ct*DNA was studied by heating a native *ct*DNA solution in a water bath at 100 °C for 10 min and then cooling in an ice−water bath immediately, accordingly to Wang et al.[54] Double-stranded *ct*DNA splits into two single-stranded *ct*DNA molecules with the opening of its double helix, so the interaction of **CuCHz** and **CuCHz**−DM$\beta$CD with denatured *ct*DNA will be different in comparison to that with double-stranded *ct*DNA. If the interaction is via intercalation, *ct*DNA accommodates the copper(II) complex in the helix, and on denaturation of the *ct*DNA helix, the intercalated molecules are released in the solution, leading an alteration in the fluorescence behavior. Table 3 displays the intensity fluorescence ratios ($F/F_0$) for **CuCHz** and **CuCHz**−DM$\beta$CD when is in the presence of different amounts of native and denatured *ct*DNA. From the table, it can be noticed a diminution of the fluorescence in denaturated *ct*DNA, which in turn supports **CuCHz** and **CuCHz**−DM$\beta$CD *ct*DNA intercalation.

The melting temperature ($T_m$) of the *ct*DNA solution, which is defined as the temperature where half of the total base pairs are unbound, is usually measured to study the interaction of an intercalator with the nucleic acid. Small molecules have an impact on the stabilization of the *ct*DNA double helix, which can be corroborated with an increase in the *ct*DNA melting


https://dx.doi.org/10.1021/acsomega.0c00275
ACS Omega 2020, 5, 6928−6936

Table 3. $F/F_0$ Data for CuCHz and CuCHz−DM$\beta$CD Complexes in Different Amounts of Native and Denatured *ct*DNA

| compound | concentration *ct*DNA (mol $L^{-1}$) | $F/F_0$ native *ct*DNA | $F/F_0$ denatured *ct*DNA |
|---|---|---|---|
| **CuCHz** | $8.0 \times 10^{-5}$ | 1.037 | 1.005 |
| | $1.6 \times 10^{-4}$ | 1.059 | 1.012 |
| | $2.4 \times 10^{-4}$ | 1.067 | 1.023 |
| | $3.2 \times 10^{-4}$ | 1.104 | 1.058 |
| | $4.0 \times 10^{-4}$ | 1.142 | 1.104 |
| **CuCHz**−DM$\beta$CD | $8.0 \times 10^{-5}$ | 1.012 | 1.007 |
| | $1.6 \times 10^{-4}$ | 1.055 | 1.048 |
| | $2.4 \times 10^{-4}$ | 1.097 | 1.072 |
| | $3.2 \times 10^{-4}$ | 1.159 | 1.112 |
| | $4.0 \times 10^{-4}$ | 1.226 | 1.147 |

temperature, probably due to increased stability of base stacking in the presence of an intercalator.[44] This temperature ($T_m$) is obtained from the midpoint of *ct*DNA melting curves, generally increasing ca. 5−8 °C for medium-sized molecules when they bind to *ct*DNA by intercalation. There is no noticeable change in temperature for nonintercalation binding. In our study, the absence of Cu(II) complexes revealed a $T_m$ of 67.9 °C; however, when Cu(II) complexes were present, the $T_m$ of *ct*DNA increased to 77.0 and 73.5 °C in the presence or absence of DM$\beta$CD, respectively (Figure 5). The $\Delta T_m$ values

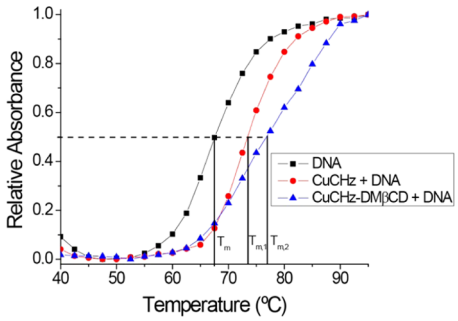


**Figure 5.** Melting curves of *ct*DNA (■) in the presence of **CuCHz** (red hexagon) and in the presence of **CuCHz**−DM$\beta$CD (blue triangle up solid). At pH 7.4, [**CuCHz**] = 25 $\mu$M and [DNA] = 50 $\mu$M.

of 9.1 and 5.6 indicate that melting temperatures correspond to those for classical intercalators.[55] We can infer that the copper(II) complex in the presence of DM$\beta$CD binds or intercalates between base pairs of double-helical *ct*DNA more efficiently, as compared to the Cu(II) complex alone.

Computational docking simulation studies of the copper(II) complex with DNA were carried out to predict the chosen binding site inside the DNA. The docked conformation of the compound with the lowest free energy and pose is shown in Figure 6. When **CuCHz** is docked into *ct*DNA, the planar ligand remains intercalated between the base pairs of DNA, forming $\pi-\pi$ interactions with the adjacent nucleotide moieties. As stated, intercalator compounds must display interactions of the $\pi-\pi$ type to achieve the expected binding mode. In our case, when the **CHz** molecule is complexed with Cu(II), it attains a planar conformation around Cu(II), which renders this molecule with the ability of such stacking interactions. Thus, according to our docking results, the chromone moiety of **CuCHz** remains intercalated to a pair of

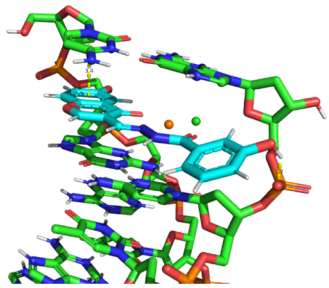

**Figure 6.** Molecular docked conformation of the copper(II) complex with DNA.

nucleobases at 3.4 Å at one side of DNA (see Figure 6). It is worth mentioning that this pose is cooperatively stabilized by several hydrogen bonds to the DNA structure. The hydroxyl group of the chromone remains to form a hydrogen bond at 1.8 Å with the G base; on the other hand, the hydroxyl group of phenol remains in a hydrogen bonding interaction with the phosphoryl hydrogen. Taking these interactions into account jointly with the strength of hydrogen bonds between G and C bases reinforced the favorable intercalated pose between **CuCHz** and DNA.

## CONCLUSIONS

The binding constant and the number of binding sites for the interaction between **CuCHz** and *ct*DNA in the absence and the presence of cyclodextrin were determined. In both cases, a single binding site in *ct*DNA for **CuCHz** was observed. The binding constant in the presence of cyclodextrin was higher, indicating that DM$\beta$CD selectively orients the drug molecule upon its binding to *ct*DNA. On the other hand, the thermodynamic results suggested that the process that drives the interaction of **CuCHz**−DM$\beta$CD with *ct*DNA could be assigned to intercalation mode. We examined the interaction of **CuCHz** to *ct*DNA and found enough pieces of evidence for its binding mode. The interaction occurrence is supported by the following findings: (i) the fluorescence studies showed an appreciable increase in the **CuCHz** emission upon the addition of *ct*DNA. (ii) A competitive reaction monitored among the EB dye, *ct*DNA, and **CuCHz** showed that the intercalated EB was displaced from the *ct*DNA−EB system by **CuCHz**. (iii) An increase in the melting temperature, $T_m$, caused by the stabilization of base stacking indicates the intercalation in the base pairs of *ct*DNA due to the presence of the copper(II) complex and (iv) the docking results of the copper(II) complex with *ct*DNA. The results presented here show also that, **CuCHz** displayed a high affinity for *ct*DNA. Furthermore, the existence of DM$\beta$CD did not affect the interaction of **CuCHz** with *ct*DNA and the inclusion complex decomposed when it binds to *ct*DNA.

## MATERIALS AND METHODS

Heptakis-2,6-*O*-dimethyl-$\beta$-cyclodextrin (DM$\beta$CD), copper(II) chloride dihydrate, 6-hydroxy-chromone-3-carboxaldehyde, 3-hydroxybenzoylhydrazine, ethidium bromide (EB), and deoxyribonucleic acid sodium salt from calf thymus (*ct*DNA) were purchased from Sigma-Aldrich. *ct*DNA was used as received without further purification. The purity of *ct*DNA was determined from optical measurements ($A_{260}/A_{280}$ > 1.8, where $A$ represents absorbance). Its concentration was determined spectrophotometrically using the molar coefficient


https://dx.doi.org/10.1021/acsomega.0c00275
ACS Omega 2020, 5, 6928−6936

value, $\varepsilon$ = 6600 L mol$^{-1}$ cm$^{-1}$. The stock solution of *ct*DNA was prepared in 5 mmol L$^{-1}$ Tris−HCl/10 mmol L$^{-1}$ NaCl buffer solution at pH 7.4 and stored in a refrigerator at 4 °C until use. The aqueous solutions used in the experiments were prepared daily from the stock solutions by appropriate dilution in the buffer solution. All solvents employed in the spectrophotometric analyses were of spectroscopic reagent grade. Deionized water from a Milli-Q system apparatus (Millipore Corp., Billerica, MA) was used throughout the experiments.

The infrared spectra were recorded by an FTIR spectrometer (Thermo iS50) equipped with a germanium attenuated total reflection (ATR) accessory, in the range of 4000−600 cm$^{-1}$, having an average of 20 spectra per analysis. The absorption spectrum was recorded on an Agilent 8453 UV−vis spectrophotometer, which is equipped with a Peltier system ±0.1 °C. Fluorescence measurements were performed on an LS55 PerkinElmer spectrofluorometer equipped with a xenon lamp source and by a Peltier temperature programmer (PerkinElmer PTP-1 Peltier system). For all experiments, 1 cm length cells were used. Mass spectra of the copper complex were recorded by a high-resolution mass spectrometer (Exactive Plus Orbitrap, ThermoFisher Scientific, Bremen, Germany). Thermogravimetric analyses were carried out from room temperature up to 800 °C at a heating rate of 10 °C min$^{-1}$ on a TA Instruments TGA Q50. The molar conductivities of the complexes in DMSO solutions ($10^{-3}$ M) were measured at room temperature using a WTW microprocessor conductivity meter LF 539. Magnetic moment measurements of the complex were carried out on a Johnson Matthey magnetic susceptibility balance using Hg[Co(SCN)$_4$] as a calibrant.

Inclusion complexes with DM$\beta$CD were obtained as described earlier.[56] For the determination of association constants ($K_a$), the concentration of **CuCHz** was 1 × $10^{-5}$ mol L$^{-1}$ and increased buffered solution of DM$\beta$CD was added. The resulting mixture was equilibrated in a Precision thermostatic shaking water bath at a determined temperature for 24 h after which the equilibrium was reached and the emission intensity was recorded.

The interaction between *ct*DNA and **CuCHz** was carried out as follows: fixed amounts of **CuCHz** (1 × $10^{-5}$ mol L$^{-1}$) in the absence and presence of DM$\beta$CD (1 × $10^{-3}$ mol L$^{-1}$) were titrated with increasing amounts of the *ct*DNA solution in the Tris−HCl/NaCl buffer solution. While measuring the absorption spectra, an equal amount of *ct*DNA was added to both the complex solution and the reference solution to eliminate the absorbance of *ct*DNA itself. In the *ct*DNA melting experiments, the absorbance of *ct*DNA (5 × $10^{-5}$ mol L$^{-1}$) at 260 nm was monitored by gradually increasing the temperature from 40 to 95 °C in the presence and absence of **CuCHz** and **CuCHz**−DM$\beta$CD (5 × $10^{-5}$ mol L$^{-1}$). The absorbance values of *ct*DNA and **CuCHz** were normalized and plotted as a function of temperature.

The intercalating effect of the copper(II) complex with the *ct*DNA−EB was studied by the gradual addition of the complex solution into the solution of *ct*DNA−EB. The *ct*DNA−EB complex was prepared by adding 0.33 $\mu$ mol L$^{-1}$ EB and 15 $\mu$ mol L$^{-1}$ *ct*DNA in the Tris−HCl/NaCl buffer solution, pH 7.4. This solution was titrated by the successive addition of 5 × $10^{-6}$ mol L$^{-1}$ stock solution of the copper(II) complex with and without cyclodextrin. The fluorescence spectra of EB bound to *ct*DNA have a maximum at 593 nm with an excitation wavelength of 500 nm with bandwidths for excitation and emission of 8 and 15 nm, respectively. The emission spectra were recorded in the 530−700 nm range.

Docking studies were carried out using AutoDock[57] (version 4.2) software. Thus, from the RCSB protein data bank, the pdb file for DNA (PDB ID: 1Z3F) was obtained. We used this crystal structure for **CuCHz**−DNA docking studies. Grid maps were calculated using AutoGrid4 centered on DM$\beta$CD defining a volume of 30 Å$^3$ with a 0.375 Å grid spacing. The AutoTors option of AutoDockTools was used to define rotatable bonds. The genetic Lamarckian algorithm was used under the following conditions: population size, 50; maximum number of evaluations, 25 000 000; maximum number of generations, 27 000; rate of mutation, 0.02; and rate of crossover, 0.08. The evaluations were performed with a default dielectric. The most stable pose of **CuCHz** was chosen according to the best docking score.

## ■ ASSOCIATED CONTENT

### Supporting Information

The Supporting Information is available free of charge at https://pubs.acs.org/doi/10.1021/acsomega.0c00275.

Synthesis and characterization of **CHz** ($^1$H NMR, $^{13}$C NMR, FTIR, MS, and TGA) and characterization of **CuCHz** (FTIR, MS, and TGA); spectroscopic studies of the inclusion complex between **CuCHz** and DM$\beta$CD; and interaction studies between the Cu(II) complex and *ct*DNA in the presence and absence of heptakis-2,6-*O*-dimethyl-$\beta$-cyclodextrin, DM$\beta$CD (PDF)

## ■ AUTHOR INFORMATION


### Corresponding Author

**Carolina Jullian** − *Departamento de Química Orgánica y Fisicoquímica, Facultad de Ciencias Químicas y Farmacéuticas, Universidad de Chile, Santiago 8380492, Chile;* orcid.org/0000-0001-6902-7170; Email: cjullian@ciq.uchile.cl

### Authors

**Horacio Gómez-Machuca** − *Departamento de Química Orgánica y Fisicoquímica, Facultad de Ciencias Químicas y Farmacéuticas, Universidad de Chile, Santiago 8380492, Chile*

**Cinthia Quiroga-Campano** − *Departamento de Química Orgánica y Fisicoquímica, Facultad de Ciencias Químicas y Farmacéuticas, Universidad de Chile, Santiago 8380492, Chile*

**Gerald Zapata-Torres** − *Departamento de Química Inorgánica y Analítica, Facultad de Ciencias Químicas y Farmacéuticas, Universidad de Chile, Santiago 8380492, Chile;* orcid.org/0000-0002-8090-1153

Complete contact information is available at: https://pubs.acs.org/10.1021/acsomega.0c00275

### Author Contributions

§H.G.-M. and C.Q.-C. contributed equally. All authors have given approval to the final version of the manuscript.


### Notes

The authors declare no competing financial interest.

## ■ ACKNOWLEDGMENTS

We thank FONDECYT grant 1160249.

## REFERENCES


(1) Zuber, G.; Quada, J. C., Jr.; Hecht, S. M. Sequence selective cleavage of a DNA octanucleotide by chlorinated bithiazoles and bleomycins. *J. Am. Chem. Soc.* **1998**, *120*, 9368−9369.

(2) Keri, R. S.; Budagumpi, S.; Pai, R. K.; Balakrishna, R. G. Chromones as a privileged scaffold in drug discovery: A review. *Eur. J. Med. Chem.* **2014**, *78*, 340−374.

(3) Gaspar, A.; Matos, M. J.; Garrido, J.; Uriarte, E.; Borges, F. Chromone: A Valid Scaffold in Medicinal Chemistry. *Chem. Rev.* **2014**, *114*, 4960−4992.

(4) Grazul, M.; Budzisz, E. Biological activity of metal ions complexes of chromones, coumarins and flavones. *Coord. Chem. Rev.* **2009**, *253*, 2588−2598.

(5) Elsayed, S. A.; Butler, I. S.; Claude, B. J.; Mostafa, S. I. Synthesis, characterization and anticancer activity of 3-formylchromone benzoylhydrazone metal complexes. *Transition Met. Chem.* **2015**, *40*, 179−187.

(6) Wang, B. D.; Yang, Z. Y.; Wang, Q.; Cai, T. K.; Crewdson, P. Synthesis, characterization, cytotoxic activities, and DNA-binding properties of the La(III) complex with Naringenin Schiff-base. *Bioorg. Med. Chem.* **2006**, *14*, 1880−1888.

(7) Li, Y.; Yang, Z. Y.; Liao, Z. C.; Han, Z. C.; Liu, Z. C. Synthesis, crystal structure, DNA binding properties and antioxidant activities of transition metal complexes with 3-carbaldehyde-chromone semicarbazone. *Inorg. Chem. Commun.* **2010**, *13*, 1213−1216.

(8) Li, Y.; Yang, Z. Y. Rare Earth Complexes with 3-Carbaldehyde Chromone(Benzoyl) Hydrazone: Synthesis, Characterization, DNA Binding Studies and Antioxidant Activity. *J. Fluoresc.* **2010**, *20*, 329−342.

(9) Wang, J.; Yang, Z. Y.; Wang, B. D.; Yi, X. Y.; Liu, Y. C. Synthesis, Characterization and DNA-binding Properties of Ln(III) Complexes with 6-Ethoxy Chromone-3Carbaldehyde Benzoyl Hydrazone. *J. Fluoresc.* **2009**, *19*, 847−856.

(10) Li, Y.; Yang, Z. DNA-binding properties and antioxidant activity of lanthanide complexes with the Schiff base derived from 3-carbaldehyde chromone and isonicotinyl hydrazine. *J. Coord. Chem.* **2010**, *63*, 1960−1968.

(11) Zülfikaroğlu, A.; Yuksektepe, C.; Celikoglu, E.; Celikoglu, U.; Idil, O. New Cu(II), Co(III) and Ni(II) metal complexes based on ONO donor tridentate hydrazone: Synthesis, structural characterization, and investigation of some biological properties. *J. Mol. Struct.* **2020**, *1199*, No. 127012.

(12) Aarjane, M.; Slassi, S.; Amine, A. Novel highly selective and sensitive fluorescent sensor for copper detection based on N-acylhydrazone acridone derivative. *J. Mol. Struct.* **2020**, *1199*, No. 126990.

(13) Reddy, A. S.; Mao, J.; Krishna, L. S.; Badavath, V. N.; Maji, S. Synthesis, spectral investigation, molecular docking and biological evaluation of Cu(II), Ni(II) and Mn(II) complexes of (E)-2-((2-butyl-4-chloro-1H-imidazol-5-yl)methylene)-N-methyl hydrazine carbothioamide ($C_{10}H_{16}N_5ClS$) and its DFT studies. *J. Mol. Struct.* **2019**, *1196*, 338−347.

(14) Li, T. R.; Yang, Z. Y.; Wang, B. D. Synthesis, characterization and antioxidative activity of new rare earth complexes of 6-hydroxy chromone-3-carbaldehyde-(4-hydroxy)benzoylhydrazone. *J. Coord. Chem.* **2007**, *60*, 597−605.

(15) Mendu, P.; Kumari, C. G. Synthesis, characterization, DNA cleavage and antimicrobial studies of ternary Co(II) complexes of 3-formylchromone Schiff bases. *J. Chem. Pharm. Res.* **2015**, *7*, 56−63.

(16) Challa, R.; Ahuja, A.; Ali, J.; Khar, R. K. Cyclodextrins in drug delivery: an updated review. *AAPS PharmSciTech* **2005**, *6*, E329−E357.

(17) Saenger, J. J. W.; Gessler, K.; Steiner, T.; Hoffmann, D.; Sanbe, H.; Koizumi, K.; Smith, S. M.; Takaha, T. Structures of the common cyclodextrins and their larger analogues beyond the doughnut. *Chem. Rev.* **1998**, *98*, 1787−1802.

(18) Szejtli, J. *Cyclodextrin Technology*; Springer: Dordrecht, Netherlands, 1988.

(19) Connors, K. A. The Stability of Cyclodextrin Complexes in Solution. *Chem. Rev.* **1997**, *97*, 1325−1358.

(20) Ye, Y.; Wang, Y.; Lou, K.; Chen, Y.; Chen, R.; Gao, F. The preparation, characterization, and pharmacokinetic studies of chitosan nanoparticles loaded with paclitaxel/dimethyl-beta-cyclodextrin inclusion complexes. *Int. J. Nanomed.* **2015**, *10*, 4309−4319.

(21) Choi, S. G.; Lee, S.; Kang, B.; Ng, C. L.; Davaa, E.; Park, J. Thermosensitive and Mucoadhesive Sol-Gel Composites of Paclitaxel/Dimethyl-beta-Cyclodextrin for Buccal Delivery. *PLoS One* **2014**, *9*, No. e109090.

(22) Grillo, R.; Silva Melo, N. F.; Moraes, C. M.; Henrique Rosa, A.; Frutuoso Roveda, J. A.; Menezes, C. M. S.; Ferreira, E. I.; Fernandes Fraceto, L. Hydroxymethylnitrofurazone: Dimethyl-beta-cyclodextrin Inclusion Complex: A Physical-Chemistry Characterization. *J. Biol. Phys.* **2007**, *33*, 445−453.

(23) Jullian, C.; Cifuentes, C.; Alfaro, M.; Miranda, S.; Barriga, G.; Olea-Azar, C. Spectroscopic characterization of the inclusion complexes of luteolin with native and derivatized [beta]-cyclodextrin. *Bioorg. Med. Chem.* **2010**, *18*, 5025−5031.

(24) Folch-Cano, C.; Olea-Azar, C.; Sobarzo-Sanchez, E.; Alvarez-Lorenzo, C.; Concheiro, A.; Otero, F.; Jullian, C. Inclusion complex of 4-hydroxycoumarin with cyclodextrins and its characterization in aqueous solution. *J. Solution Chem.* **2011**, *40*, 1835−1846.

(25) Jullian, C.; Miranda, S.; Zapata-Torres, G.; Mendizábal, F.; Olea-Azar, C. Studies of Inclusion Complexes of natural and modified cyclodextrin with (+) catechin by NMR and Molecular Modeling. *Bioorg. Med. Chem.* **2007**, *15*, 3217−3224.

(26) Folch-Cano, C.; Guerrero, J.; Speisky, H.; Jullian, C.; Olea-Azar, C. NMR and molecular fluorescence spectroscopic study of the structure and thermodynamic parameters of EGCG/ $\beta$-cyclodextrin inclusion complexes with potential antioxidant activity. *J. Inclusion Phenom. Macrocyclic Chem.* **2014**, *78*, 287−298.

(27) Jullian, C.; Orosteguis, T.; Pérez-Cruz, F.; Sánchez, P.; Mendizábal, F.; Olea-Azar, C. Complexation of morin with three kinds of cyclodextrin. A thermodynamic and reactivity study. *Spectrochim. Acta, Part A* **2008**, *71*, 269−275.

(28) Cifuentes, T.; Cayupi, J.; Celis-Barros, C.; Zapata-Torres, G.; Ballesteros, R.; Ballesteros-Garrido, R.; Abarca, B.; Jullian, C. Spectroscopic studies of the interaction of 3-(2-thienyl)-[1,2,3]-triazolo[1,5-a]pyridine with 2,6-dimethyl-$\beta$-cyclodextrin and ctDNA. *Org. Biomol. Chem.* **2016**, *14*, 9760−9767.

(29) Ibrahim, M. S.; Shehatta, I. S.; Al-Nayeli, A. A. Voltammetric studies of the interaction of lumazine with cyclodextrins and DNA. *J. Pharm. Biomed. Anal.* **2002**, *28*, 217−223.

(30) Sameena, Y.; Enoch, I. V. M. V. The influence of $\beta$-cyclodextrin on the interaction of hesperetin and its bismuth (III) complex with calf thymus DNA. *J. Lumin.* **2013**, *138*, 105−116.

(31) Chandrasekaran, S.; Sameena, Y.; Enoch, I. V. M. V.; Santhanam, V. Binding of the Host−Guest complex of 7-aminoflavone/$\beta$-cyclodextrin with calf thymus DNA: A spectroscopic and Molecular Docking study. *J. Solution Chem.* **2014**, *43*, 1132−1146.

(32) Chandrasekaran, S.; Sameena, Y.; Enoch, I. V. Tuning the binding of coumarin 6 with DNA by molecular encapsulators: effect of $\beta$-cyclodextrin and C-hexylpyrogallol[4]arene. *J. Mol. Recognit.* **2014**, *27*, 640−652.

(33) Xu, D.; Wang, X.; Ding, L. Spectroscopic studies on the interaction of $\gamma$-cyclodextrin−daunorubicin inclusion complex with herring sperm DNA. *Carbohydr. Polym.* **2011**, *83*, 1257−1262.

(34) Krzak, A.; Swiech, O.; Majdecki, M.; Bilewicz, R. Complexing daunorubicin with b-cyclodextrin derivative increases drug intercalation into DNA. *Electrochim. Acta* **2017**, *247*, 139−148.

(35) Jabeen, E.; Janjua, N. K.; Hemeed, S. $\beta$-Cyclodextrin assisted solubilization of Cu and Cr complexes of flavonoids in aqueous medium: A DNA-interaction study. *Spectrochim. Acta, Part A* **2014**, *128*, 191−196.

(36) Usman, M.; Zaki, M.; Khan, R. A.; Alsalme, A.; Ahmad, M.; Tabassum, S. Coumarin centered copper(II) complex with appended-imidazole as cancer chemotherapeutic agents against lung cancer:




https://dx.doi.org/10.1021/acsomega.0c00275
*ACS Omega* 2020, 5, 6928−6936

molecular insight via DFT-based vibrational analysis. *RSC Adv.* **2017**, *7*, 36056−36071.
(37) Saif, M.; El-Shafiy, H. F.; Mashaly, M. M.; Eid, M. F.; Nabeel, A. I.; Fouad, R. Synthesis, characterization, and antioxidant/cytotoxic activity of new chromone Schiff base nano-complexes of Zn(II), Cu(II), Ni(II) and Co(II). *J. Mol. Struct.* **2016**, *1118*, 75−82.
(38) Venkateswarlu, K.; Ganji, N.; Daravath, S.; Kanneboina, K.; Rangan, K.; Shivaraj. Crystal structure, DNA interactions, antioxidant and antitumor activity of thermally stable Cu(II), Ni(II) and Co(III) complexes of an N,O donor Schiff base ligand. *Polyhedron* **2019**, *171*, 86−97.
(39) Philip, J. E.; Antony, S. A.; Eeettinilkunnathil, S. J.; Kurup, M. R. P.; Velayudhan, M. P. Design, synthesis, antimicrobial and antioxidant activity of 3-formyl chromone hydrazone and their metal (II) complexes. *Inorg. Chim. Acta* **2018**, *469*, 87−97.
(40) Qi, G. F.; Yang, Z. Y.; Qin, D. D. Synthesis, Characterization and DNA-Binding Properties of the Cu(II) Complex with 7-Methoxychromone-3-carbaldehyde-benzoylhydrazone. *Chem. Pharm. Bull.* **2009**, *57*, 69−73.
(41) Benesi, H. A.; Hildebrand, J. H. A spectrophotometric investigation of the interaction of iodine with aromatic hydrocarbons. *J. Am. Chem. Soc.* **1949**, *71*, 2703−2707.
(42) Liu, L.; Guo, Q. X. The Driving Forces in the Inclusion Complexation of Cyclodextrins. *J. Inclusion Phenom. Macrocyclic Chem.* **2002**, *42*, 1−14.
(43) Rehman, Z.; Shah, A.; Muhammed, N.; Ali, S.; Qureshi, R.; Meetsma, A.; Butler, I. S. Synthesis, spectroscopic characterization, X-ray structure and evaluation of binding parameters of new triorganotin(IV) dithiocarboxylates with DNA. *Eur. J. Med. Chem.* **2009**, *44*, 3986−3993.
(44) Perdisatt, L.; Moqadasi, S.; O'Neill, L.; Hessman, G.; Ghion, A.; Mushtaq Warraich, M. Q.; Casey, A.; O'Connor, C. Synthesis, characterization and DNA intercalation studies of regioisomers of ruthenium (II) polypyridyl complexes. *J. Inorg. Biochem.* **2018**, *182*, 71−82.
(45) Sirajuddin, M.; Ali, S.; Badshah, A. Drug−DNA interactions and their study by UV−Visible, fluorescence spectroscopies and cyclic voltammetry. *J. Photochem. Photobiol., B* **2013**, *124*, 1−19.
(46) Pakravan, P.; Masoudian, S. Study on the Interaction between Isatin-$\beta$-Thiosemicarbazone and Calf Thymus DNA by Spectroscopic Techniques. *Iran. J. Pharm. Res.* **2015**, *14*, 111−123.
(47) Huang, Y.; Lu, Q. S.; Zhang, J.; Zhang, Z. W.; Zhang, Y.; Chen, S. Y.; Li, K.; Tan, X. Y.; Lin, H. H.; Yu, X. Q. DNA cleavage by novel copper (II) complex and the role of b-cyclodextrin in promoting cleavage. *Bioorg. Med. Chem.* **2008**, *16*, 1103−1110.
(48) Ross, P. D.; Subramanian, S. Thermodynamics of protein association reactions: Forces contributing to stability. *Biochemistry* **1981**, *20*, 3096−3102.
(49) Qiao, C.; Bi, S.; Sun, Y.; Song, D.; Zhang, H.; Zhou, W. Study of interactions of anthraquinones with DNA using ethidium bromide as a fluorescence probe. *Spectrochim. Acta, Part A* **2008**, *70*, 136−143.
(50) Goftar, M. K.; Kor, N. M.; Kor, Z. M. DNA intercalators and using them as anticancer drugs. *Int. J. Adv. Biol. Biomed. Res.* **2014**, *2*, 811−822.
(51) Paul, A.; Bhattacharya, S. Chemistry and biology of DNA-binding small molecules. *Curr. Sci.* **2012**, *102*, 212−231.
(52) Haq, I. Part II: The thermodynamics of drug−bipolymer interaction thermodynamics of drug−DNA interactions. *Arch. Biochem. Biophys.* **2002**, *403*, 1−15.
(53) Yang, H.; Wang, X. M. Spectroscopic studies on the interaction of $\beta$-cyclodextrin-8-Hydroxyquinoline inclusion complex with herring sperm DNA. *J. Mol. Struct.* **2013**, *1036*, 51−55.
(54) Wang, B.; Yang, Z. Y.; Crewdson, P.; Wang, D. Synthesis, crystal structure and DNA-binding studies of the Ln(III) complex with 6-hydroxychromone-3-carbaldehyde benzoyl hydrazine. *J. Inorg. Biochem.* **2007**, *101*, 1492−1504.
(55) Zhou, X.; Zhang, G.; Wang, L. Probing the binding mode of psoralen to calf thymus DNA. *Int. J. Biol. Macromol.* **2014**, *67*, 228−237.
(56) Jullian, C.; Fernández-Sandoval, S.; Rojas-Aranguiz, M.; Gómez-Machuca, H.; Salgado-Figueroa, P.; Celis-Barros, C.; Zapata-Torres, G.; Adam, R.; Abarca, B. Detecting Ni(II) in aqueous solution by 3-(2-pyridyl)-[1,2,3]triazolo[1,5-a]pyridine and dimethyl–cyclodextrin. *Carbohydr. Polym.* **2014**, *107*, 124−131.
(57) Morris, G. M.; Huey, R.; Lindstrom, W.; Sanner, M. F.; Belew, R. K.; Goodsell, D. S.; Olson, A. J. Autodock4 and AutoDockTools4: automated docking with selective receptor flexiblity. *J. Comput. Chem.* **2009**, 2785−2791.


https://dx.doi.org/10.1021/acsomega.0c00275
*ACS Omega* 2020, 5, 6928−6936